Contents lists available at ScienceDirect

MethodsX

journal homepage: www.elsevier.com/locate/methodsx

A modular, cost-effective, versatile, open-source operant box solution for long-term miniscope imaging, 3D tracking, and deep learning behavioral analysis

Nicholas J. Beacher [a],*, Jessica Y. Kuo [a], Miranda Targum [b], Michael Wang [a], Kayden A. Washington [c], Giovanna Barbera [a], Da-Ting Lin [a]

[a] Intramural Research Program, National Institute on Drug Abuse, 333 Cassell Drive, Baltimore, MD 21224, United States
[b] Penn Memory Center, University of Pennsylvania, Philadelphia, PA, United States
[c] The Feinberg School of Medicine at Northwestern University, Chicago, IL, United States

ARTICLE INFO

ABSTRACT

In this procedure we have included an open-source method for a customized operant chamber optimized for long-term miniature microscope (miniscope) recordings.

- The miniscope box is designed to function with custom or typical med-associates style accessories (e.g., houselights, levers, etc.).
- The majority of parts can be directly purchased which minimizes the need for skilled and time-consuming labor.
- We include designs and estimated pricing for a single box but it is recommended to build these in larger batches to efficiently utilize bulk ordering of certain components.

Specifications table

Subject area:	Neuroscience
More specific subject area:	Behavioral Neuroscience
Name of your method:	The Miniscope Box
Name and reference of original method:	n/a
Resource availability:	https://github.com/NJBeacher/NJBeacher.github.io.git
	See tables 1, 2, and 3 for detailed resources

Method details

Miniaturized microscope (miniscope) imaging is an exciting new frontier in behavioral neuroscience. Miniscopes can be combined with implantable Gradient Index (GRIN) lenses [1] and can be used for recording hundreds of neurons in mice [2–12] and rats [13–16] longitudinally. Deep learning tools can be used to automatically identify neural associations with behaviors [6] for high impact in vivo behavioral neuroscience. However, typical operant boxes require modifications to accommodate necessary imaging experiments (e.g., a raised or completely open ceiling) and require specialized equipment such as motorized commutators [17] or mounted cameras for multi-dimensional behavioral recording [18–21]. Modifying operant chambers to suit these needs can potentially degrade their integrity and may not be designed to house rats for 24 h/day.

---

* Corresponding author.
E-mail address: Nicholas.beacher@nih.gov (N.J. Beacher).
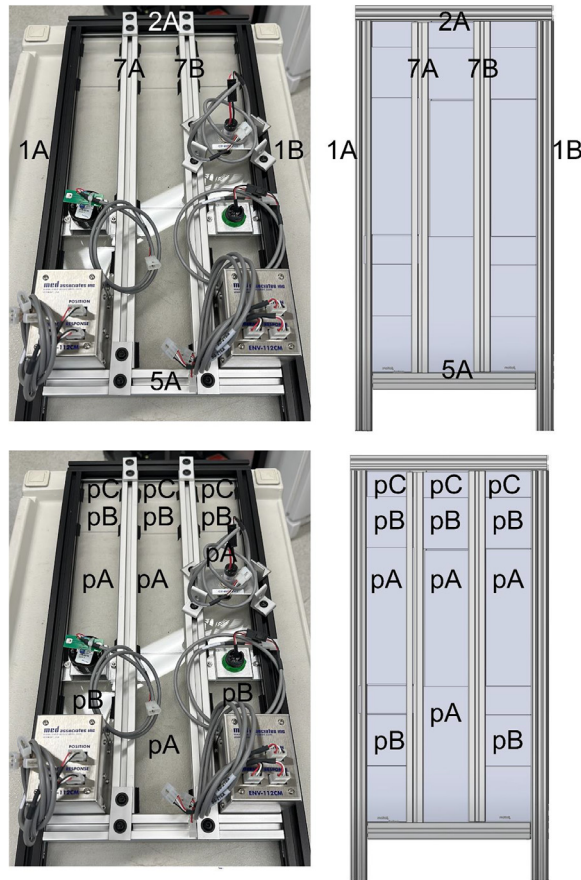
Fig. 1. Left Side Views of the operant box. Top: Labeled rail diagram of the SolidWorks design (Right) and real world (Left) section of the box. Bottom: Acrylic diagram of the SolidWorks design (Right) and real world (Left) section of the box. Also shown are the inserted Med Associates ™ commercially obtainable levers, houselights, etc. that can easily be inserted.

We have designed a completely custom operant chamber designed to address these challenges. Our design is tall, resilient, and functions with custom [22] or commercial (e.g., Med Associates, Inc. (St. Albans, VT)) operant components that researchers may already have in-house. Furthermore, it is completely modular to easily accommodate changes or adaptations such as affixing cameras (internally and/or externally), latching components (e.g., houselight) outside the chamber to prevent climbing, 100% transparent 'climb-resistant' walls, and an optional acrylic flooring for bottom-up video recording. We include both completely detailed instructions and a companion video for full construction of the main chamber (see https://youtu.be/-rvy9stXxhE?t=1) (Figs. 1–4) and also include completely detailed instructions for an attachable social chamber (Figs. 5 and 6) for social self-administration [23–25].

All options are customizable and avoid interference with video recording or commutators. We include all SolidWorks designs, a detailed construction walkthrough, and a detailed breakdown of components and cost. We have prioritized ease of construction, modular capabilities, and long-term miniscope imaging. All SolidWorks designs for the box are located here: https://github.com/NJBeacher/NJBeacher.github.io.git and are also depicted in Tables 1 and 2. The SolidWorks designs can be uploaded into SolidWorks (or similar) software for modification as necessary. These designs could also be used for 3D printing; however, it is only suggested to use a metal printing service as the plastic used in the printing process can easily be chewed through by rats. The T-slotted framing rails (and accessory components) can also be ordered through additional sources (e.g., Thorlabs, AutomationDirect, Grainger) and acrylic can also be ordered through any typical laser cutting acrylic service (e.g., TAP plastics, ShapesPlastics, etc.).

Tables 1–3 also include all prices estimated for setting up these boxes. A single commercial Med Associates operant chamber with commercial components equates to 10,648. For our custom operant chambers, it is estimated that a single box without Med Associates commercial components will cost 2272.61 (231.92 for rails, 1500.00 for acrylic, and 540.69 for accessories). A single custom box with Med Associates commercial components (i.e. levers, house lights, cue generators) costs 9910.61.

10 commercial Med Associates operant chambers with commercial components costs 85,177. For our chambers, 10 of our custom boxes without commercial components cost 7720, and 10 of our custom boxes with commercial components cost 52,606. We suggest building at least 10 of our custom operant boxes due to scalable costs: acrylic is 1500 for 1 or 10 boxes due to ordering values, the "perforated barrier" can be used for up to 10 boxes, and all other components in Table 3 that can be reused are noted with
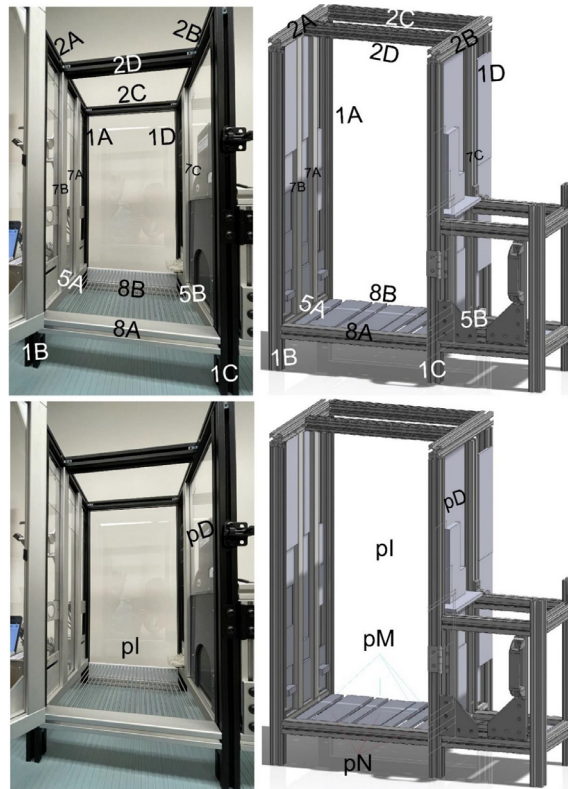
Fig. 2. Main chamber (Inner View). Top: Labeled rail diagram of the SolidWorks design (Right) and real world (Left) section of the inner box. Bottom: Acrylic diagram of the SolidWorks design (Right) and real world (Left) section of the inner box. Also shown is a Med Associates gridfloor can be installed as shown in the real photos. Alternatively, acrylic can be used for flooring as shown in the SolidWorks schematics. Bottom-up camera views can be useful for certain situations which highlights flexibilities offered by this design.

an *. The majority of these costs come from the commercial components. Open source and 3D-printed external options to replace commercially available operant components are available that can dramatically reduce costs as well [22,26]. If adding dual-cameras, cables, network cards, and optical posts, the additional cost is estimated at 1141.88 per box.

Constructing the open-source operant box

Please see the attached instructional video (see https://youtu.be/-rvy9stXxhE?t=1) for a completely detailed walkthrough of each step.

1. Left wall of main chamber (see 0:13 https://youtu.be/-rvy9stXxhE?t=13)
   a. Orient rail 5A such that the smooth face will be facing the interior of the operant chamber. In this orientation, 5A is positioned upright. Measure and mark 3" from either end of 5A.
   b. Slide one end of two straight brackets onto the slotted face, which is towards the outside of the box and opposite of the smooth face of 5A, and secure.
   c. Using these straight brackets, secure 7A and 7B on-center at the 3" marks such that there are three empty columns of approximately even size and the smooth face is towards the inside of the chamber.
   d. Measure 2.5" from the bottom end of 1A and 1B. Attach two corner concealed brackets to the bottom slotted face of 5A. Secure 5A to 1A and 1B such that the bottom face of 5A is elevated 2.5" from the work surface. Ensure 1A is the back left corner and 1B is the front left corner of the operant chamber.
   e. Lay the rails down such that the interior face is on the work surface (Fig. 1; Top). Slide a lever assembly between 1A and 7A followed by acrylic pB, a cue speaker, and acrylic pA, pB, and pC. Between 7A and 7B, insert two pA, one pB, and one pC acrylic piece. For the final column between 7B and 1B, insert a lever assembly, pB, a cue light, pA, pB, and one pC piece (Fig. 1; Bottom).
   f. Slide two corner brackets down rail 7B and another two corner brackets down rail 1B, leaving one bolt hole on each corner bracket empty. These corner brackets will create a frame to hold the houselight after this face of the operant chamber is completed.
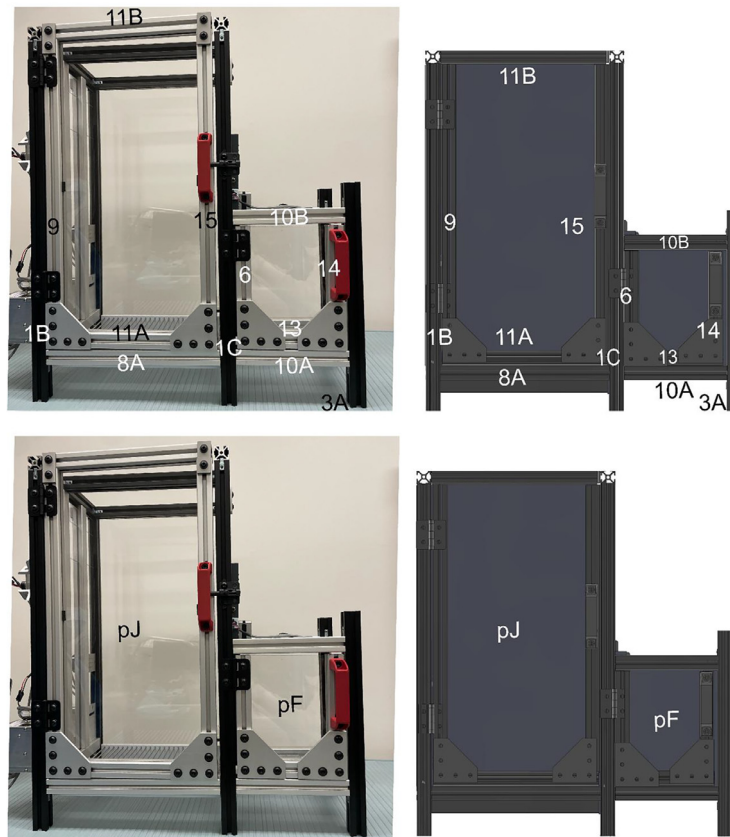
Fig. 3. Front outer view of main chamber and attached social chamber. Top: Labeled rail diagram of the SolidWorks design (Right) and real world (Left) section of the main chamber and attached social chamber. Bottom: Acrylic diagram of the SolidWorks design (Right) and real world (Left) section of the main chamber and attached social chamber.

    g. Secure two corner concealed brackets onto the bottom face of rail 2A. The brackets should end exactly 7/8" into each side of 2A. Reverse the remaining single tension screws on both corner concealed brackets. Slide two straight brackets onto the outer face of rail 2A, 4" on center from either end of 2A, adjacent to the bottom face with concealed brackets.

    h. Secure the corner concealed brackets to 1A and 1B in addition to securing the straight brackets to 7A and 7B. Tighten all brackets and insert rubber gaskets to tension the outer face of acrylic walls against rails 1A, 7A, 7B, and 1B.

    i. Secure the houselight into the corner bracket frame.

2. Right wall of main chamber (see 6:35 https://youtu.be/-rvy9stXxhE?t=395)

    a. Measure 2.5" from the bottom end of 1C and 1D. Ensure 1D is the back right corner and 1C is the front right corner of the operant chamber.

    b. Orient rail 5B so that the smooth face is facing the operant chamber's interior. Attach two corner concealed brackets to the bottom face of 5B.

    c. Measure 3" from end closest to 1D of rail 5B Slide a straight bracket onto 5B and secure on center at the 3" mark.

    d. Secure 5B to 1C and 1D such that the bottom face of 5B is 2.5" from the bottom of 1C and 1D (Fig. 2; Top).

    e. Secure 7C to 5B using the straight bracket. Orient rail 7C so that the smooth face is facing the operant chamber's interior.

    f. Insert acrylic pD, pH, and pK into the larger section between rails 1C and 7C.

    g. Elevate the frame to insert the food port, acrylic pB, a Med Associates pellet dispenser, followed by acrylic pA and two pC pieces.

    h. Secure two corner concealed brackets onto the bottom face of rail 2B. Reverse the remaining single tension screws on both corner concealed brackets.

    i. Slide one straight bracket on the outer face of rail 2B.

    j. Secure the corner concealed brackets to 1C and 1D in addition to securing the straight bracket to 7C. Tighten all brackets and insert rubber gaskets to tension the outer face of acrylic walls against rails 1C, 7C, and 1D.

    k. Secure the deadbolt with locking grooves facing downwards onto rail 1C.

3. Main chamber floor (see 10:00 https://youtu.be/-rvy9stXxhE?t=600)

    a. Orient 8A such that the flat face is towards the top of the operant chamber. Attach corner concealed brackets to the bottom side of rail 8A.
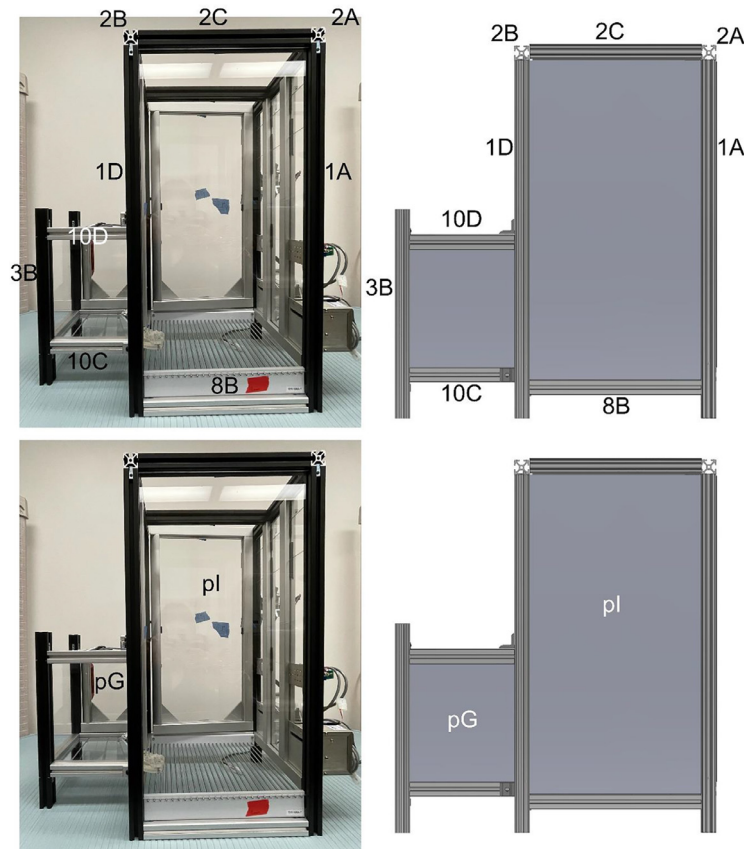
Fig. 4. Back outer view of main chamber. Top: Labeled rail diagram of the SolidWorks design (Right) and real world (Left) section of the backside of the box and attached social chamber. Bottom: Acrylic diagram of the SolidWorks design (Right) and real world (Left) section of the backside of the box and attached social chamber.

    b. Arrange the grid floor such that the exposed rail ends are pointed out of the back of the chamber and the rails are towards the top end of the plastic endpiece. Secure two screws into the holes of the grid floor and loosely screw in the nuts. The nuts should be facing the front of the chamber.

    c. Slide the grid floor into the interior slotted face of 8A. Continue to tighten the screws until secure.

    d. Secure the right side of rail 8A to rail 1C with a corner concealed bracket. The bottom side of rail 8A should be at the 2.5" mark of rail 1C.

    e. Orient rail 8B so that the flat face is towards the bottom. Attach two corner concealed brackets to either end of the top slotted face of rail 8B. Join rail 8B to rail 1D. The plastic edge of the grid floor should rest on the corner concealed brackets on rail 8B (Fig. 2; Top).

    f. Lift the left wall of the operant chamber assembly and attach rail 1A to rail 8B and rail 1B to rail 8A. Tighten all brackets and connections (Fig. 2; Top).

4. Main chamber back wall and ceiling (see 13:20 https://youtu.be/-rvy9stXxhE?t=800)

    a. Slide in acrylic pI between rails 1A and rails 1D so that it is sitting on top of the exposed rail ends (Fig. 2; Bottom, Fig. 4; Bottom).

    b. Attach rail 2C on top of acrylic pI with two corner concealed brackets.

    c. Using two corner concealed brackets, secure rail 2D to rails 2A and 2B such that it provides extra support to the chamber (Fig. 2; Top). The exact location can vary depending on experimental design.

    d. Alternatively, if not using the med-associates flooring, then rails 8A and 8B can be lowered 1" to fit the back wall appropriately.

5. Main chamber door (see 14:38 https://youtu.be/-rvy9stXxhE?t=878)

    a. Secure the two corner surface brackets to either end of 11A such that the surface brackets are facing outwards and the two smooth faces of 11A are towards the bottom and inside of the chamber.

    b. Secure rail 15 to the right side of 11A using the corner surface bracket. Ensure that rail 15 is oriented such that one slotted face is towards the outside of the box and the other allows for an acrylic wall to slide into the door frame.

    c. Attach rail 9 to 11A using the other corner surface bracket with the flat face of rail 9 on the inside of the operant chamber (Fig. 3; Top).
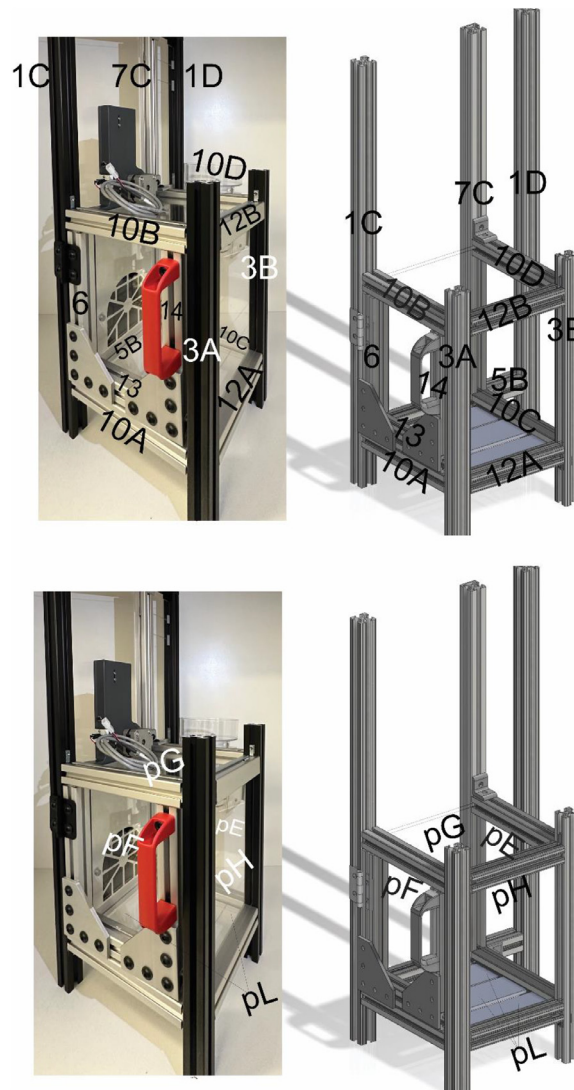
Fig. 5. Social chamber and right wall of main chamber. Top: Labeled rail diagram of the SolidWorks design (Right) and real world (Left) section of the right wall with the attachable social chamber. Bottom: Acrylic diagram of the SolidWorks design (Right) and real world (Left) section of the right wall with the attachable social chamber. Also shown is an inserted social guillotine door (See Fig. 6 for adjustments).

    d. Orient the hinge joints to face outwards and secure the right halves of two hinges onto rail 9 and a handle onto rail 15.
    e. Slide and secure the handle onto rail 15 at a comfortable height.
    f. Slide acrylic wall pJ into place and attach 11B using two straight brackets on the front face and secure to 9 and 15 (Fig. 3).
    g. Ensure rail 11B is oriented such that one flat face is towards the inside of the box and one is towards the top.
    h. Slide the door up from the bottom of rail 1B. Tighten the hinge to rail 1B (Fig. 3; Top).
    i. Adjust the height of the deadbolt on rail 1C if necessary (Fig. 3).

Constructing the optional attachable social chamber

    The following instructions explain how to make the social chamber (Fig. 5), which is attached to the right wall of the main chamber (Figs. 3 and 4). Instructions for the right wall of the main chamber are modified to accommodate the social chamber and are explained below.

    1. Social chamber
        a. Measure 2.5" and 11.75" from the bottom of rail 3A. Rail 3A is the right front leg of the social chamber.
        b. Slide two corner concealed brackets on adjacent faces at the 2.5" mark. Secure rails 10A and 12A at the 2.5" mark such that the bottom face of rails 10A and 12A are at the marks. Confirm the smooth face of rail 10A is facing up, and the smooth
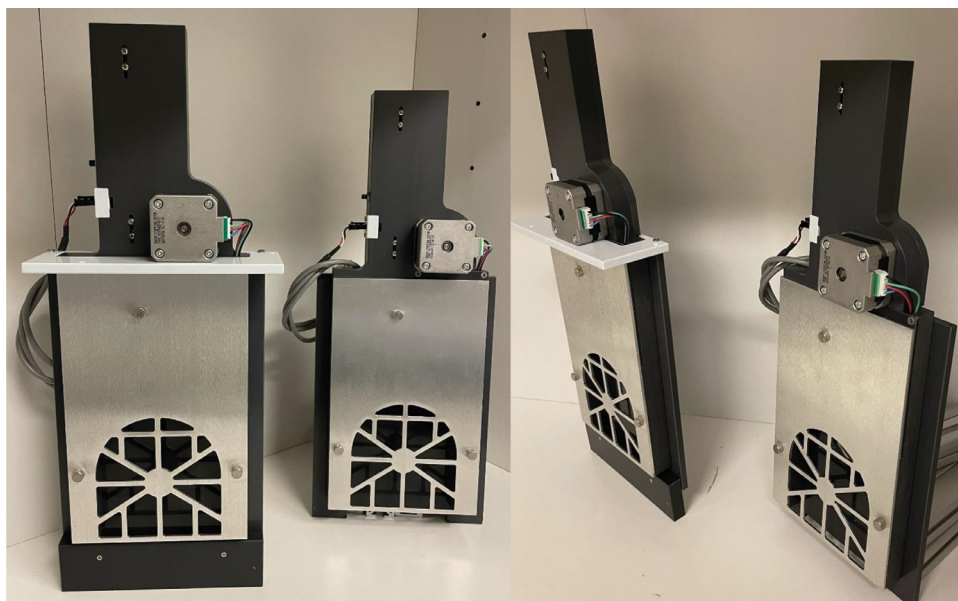
Fig. 6. Social guillotine door adjustments. Adjustments made to the social guillotine door prior to inserting into the main box. The original door includes a removable white plastic part and a removable gray plastic part. Shown here are before and after comparisons of the social guillotine door configurations.

Table 1
Information regarding the rails used for the box and social chamber.

Label	Description	Solid Works Part	Rail Length (inches)	Quantity/ Box	Part ID	Cost/Inch	Total Cost Per Box
1A, 1B, 1C, 1D	Square, 4-Slot	24in47065T801_T-Slotted Framing	24	4	47065T807	0.77	73.92
2A, 2B, 2C, 2D	Square, 4-Slot	11_5in47065T801_T-Slotted Framing rail	11.5	4	47065T807	0.77	35.42
3A, 3B	Square, 4-Slot	14_47065T801_T-Slotted Framing	14	2	47065T807	0.77	21.56
4	Square, 4-Slot	6in_47065T801_T-Slotted Framing	6	1	47065T807	0.77	4.62
5A, 5B	Square, 3-Slot	9_5in6575N217_T-Slotted Framing Rail	9.5	2	6575N217	0.54	10.26
6	Square, 3-Slot	6_75in6575N217_T-Slotted Framing Rail	6.75	1	6575N217	0.54	3.65
7A, 7B, 7C	Square, 3-Slot	20_5in6575N217_T-Slotted Framing Rail	20.5	3	6575N217	0.54	11.21
8A, 8B	Square, 3-Slot	11_5in6575N217_T-Slotted Framing Rail	11.5	2	6575N217	0.54	12.42
9	Square, 3-Slot	19_5in6575N217_T-Slotted Framing Rail	19.5	1	6575N217	0.54	10.53
10A, 10B, 10C, 10D	Square, 3-Slot	7in_6575N217_T-Slotted Framing Rail	7	4	6575N217	0.54	15.12
11A, 11B	Square, 2-Slot	11_25in47065T846_T-Slotted Framing	11.25	2	47065T846	0.50	11.25
12A, 12B	Square, 2-Slot	6in_47065T846_T-Slotted Framing	6	2	47065T846	0.50	6.00
13	Square, 2-Slot	6_75in6575N217_T-Slotted Framing Rail	6.75	1	47065T846	0.50	3.38
14	Round, 2-Slot	6_75_6575N218_T-Slotted Framing Rail	6.75	1	6575N218	0.48	3.24
15	Round, 2-Slot	19_5in6575N218_T-Slotted Framing Rail	19.5	1	6575N218	0.48	9.36

Dimensions, descriptions, and pricing for rails (source: McMaster-Carr). SolidWorks designs were modified based off designs available in the links for each Part ID. All SolidWorks designs for rails are included: https://github.com/NJBeacher/NJBeacher.github.io.git. The total cost of rails for each box is estimated to be 231.92 from the McMaster source. Please note, this cost does not scale with additional boxes like the acrylic cost scales.

faces of rail 12A are facing the chamber's interior and up. Rail 10A will be at the front bottom of the chamber, and rail 12A is the bottom right side of the chamber. (Fig. 5; Top).

c. Using a corner concealed bracket, secure rail 10B on center at the 11.75″ mark of rail 3A so that rail 10B is parallel to rail 10A and the smooth face of rail 10B is facing down, mirroring rail 10A.

d. Using a corner concealed bracket, secure rail 12B on center at the 11.75″ mark of rail 3A so that rail 12B is parallel to rail 12A and the smooth faces of rail 12B are facing the chamber's interior and down, mirroring rail 12A.

e. Measure 2.5″ and 11.75″ from the bottom of rail 3B. Using a corner concealed bracket, secure rail 10C to rail 3B such that the bottom of rail 10C is at the 2.5″ mark and the smooth face of rail 10C is facing up (Fig. 5; Top, Fig. 3; Top).

f. Using a corner concealed bracket, secure rail 10D to rail 3B such that rail 10D is on center at the 12″ mark and the smooth face of rail 10D is facing down, mirroring rail 10C (Fig. 2; Top).

g. Slide in acrylic pH between rails 12A and 12B (Fig. 5; Bottom).

h. Secure rail 3B to rails 12A and 12B with two corner concealed brackets, such that rail 12B is perpendicular to rail 10D and rail 12A is perpendicular to rail 10C.

Table 2

Information regarding the acrylic & custom parts used for the box and social chamber.

Label	SolidWorks Part	Width (inches)	Length (inches)	Thickness (inches)	Quantity/ Box
pA	pA	3	8	0.1875	5
pB	pB	3	3	0.1875	6
pC	pC	3	1.50	0.1875	4
pD	pD	6.5	11.75	0.1875	1
pE	pE	7.5	8	0.1875	1
pF	pF	5.375	7.125	0.1875	1
pG	pG	6.75	6.5	0.1875	1
pH	pH	6.5	7.875	0.1875	1
pI	pI	12	21.375	0.1875	1
pJ	pJ	9.875	19.75	0.1875	1
pK	pK	6.5	1	0.1875	1
pL	pL	6.5	2	0.1875	3
pM	pM	10	1	0.1875	4
pN	pN	10	2	0.1875	3
side	side	n/a	n/a	n/a	2
foodport	food_port_R001	n/a	n/a	n/a	1

Acrylic dimensions for construction of the main box and attachable social chamber. It is recommended to order larger quantities of cut acrylic (this scales with cost). Different companies will charge different rates for the amount ordered of each cut size. This will typically be cut from a single larger sheet. It is recommended to adjust this for each website to maximize the total 'cut' pieces which can be made from a single order. For 1 box we estimated a cost of ~1500, however, we estimate this cost to be 1585 for 10 boxes when maximizing this ordering process through ACME-plastics. All SolidWorks designs for acrylic are here: https://github.com/NJBeacher/NJBeacher.github.io.git. Also shown are the custom designed foodports and side pieces which are included in the GitHub page.

  i. Slide in 2 pK and 2 pL slats with the pL slats closer to the main chamber/guillotine and secure them between rails 10A and 10C of the social chamber using pieces cut from the antislip cover. This is the floor of the social chamber (Fig. 5; Bottom).

  j. Secure the deadbolt with locking grooves facing downwards onto rail 3A.

2. Right wall of main chamber

  a. Measure 2.5" from the bottom end of 1C and 1D. Orient rail 5B so that the smooth face is facing the operant chamber's interior.

  b. Attach two corner concealed brackets to the bottom face of 5B. Slide a corner bracket onto 5B. Secure 5B to 1C and 1D such that the bottom face of 5B is elevated 2.5″ from the work surface (Fig. 5; Top). Ensure 1D is the back right corner and 1C is the front right corner of the operant chamber.

  c. Secure the deadbolt with locking grooves facing downwards onto rail 1C.

3. Securing social chamber to right wall of main chamber

  a. Slide in acrylic pG between rails 10B and 10D. This is the top of the social chamber (Fig. 5; Bottom).

  b. Slide a corner concealed bracket into rails 10A and 10B.

  c. Slide the social chamber starting from the bottom of rail 1C of the operant.

  d. chamber, and secure rail 10A, and rail 10B of the social chamber to rail 1C using the corner concealed brackets (Fig. 3; Top).

  e. The bottom face of rail 10A should be at the 2.5″ mark of rail 1C. Using the corner bracket that was attached to rail 5B, secure the outside face of rail 10C of the social chamber to rail 5B of the operant chamber (Fig. 5; Top).

  f. Slide acrylic pE between rails 10C and 10D of the social chamber.

  g. Place rail 7C vertically on top of rail 5B, with the smooth face of rail 7C facing the operant chamber's interior. Using a corner bracket, secure rail 10D to rail 7C.

  h. Place the social guillotine door between rails 1C and 7C so that it is sitting on rail 5B. Slide acrylic pD between rails 1C and 7C and in front of the social guillotine door so that pD is touching the top of the chamber (Fig. 2; Bottom). See Appendix and Fig. 6 for necessary modifications to the social guillotine door prior to installation.

  i. Between rails 7C and 1D, slide a food port, acrylic pB, pA, and 3 pC's.

  j. Place rail 2B on top of rails 1C and 1D. Secure 2B to 1C with a corner concealed bracket. Reverse the tension screw of the corner concealed bracket that attaches to rail 1C.

  k. Secure 2B and 1D with a corner concealed bracket and reverse the tension screw that attaches to rail 1D.

  l. Using a straight bracket, secure rails 2B and 7C on the outer face of the chamber.

4. Social chamber door

  a. Attach two surface corner brackets to the outer facing side of rail 13. The smooth faces of rail 13 will face the social chamber's interior and the ground.

  b. Using the surface corner brackets, secure rail 6 and rail 14 to the edges of the slotted face of rail 13. Attach rails 6 and 14 so that they are both perpendicular to rail 13, rail 6 is on the left side of rail 13 with its smooth side facing inside the chamber, and rail 14 is on the right side of rail 13 (Fig. 3).

Table 3

Additional box components, cables, cameras, med associates components.

Name	Description	Manufacturer	Quantity/ Box	Part ID	Cost/ Part	Cost/ Box
Rail-to-Rail Hinge	Main box/Social door hinges	McMaster-Carr	3	47065T347	19.39	58.17
Corner Bracket	Used to mount external stimuli *Helps prevent climbing	McMaster-Carr	6	47065T236	7.92	47.52
Straight Surface Bracket	Attach rails (externally)	McMaster-Carr	7	47065T255	9.23	64.61
Pull Handle	Door handles for main/social	McMaster-Carr	2	47065T595	12.84	25.68
Antislip Cover**	Interspaces acrylic floors/gasket. Optional if using med-associates flooring without a social chamber attachment	McMaster-Carr	1	47065T362	19.01	19.01
Panel Gasket *	Used as gasket to keep acrylic panels and med-associates attachments firmly in place.	McMaster-Carr	1	7437N11	8.21	8.21
Corner Concealed Bracket	Attach rails (internally)	McMaster-Carr	20	5537T315	3.08	61.60
Corner Surface Bracket	Attaches rails at bottom of doors	McMaster-Carr	4	47065T267	11.60	46.40
PVC Plastic Tubing*	Extend length of med-associates feeder hoppers	McMaster-Carr	1	9446K71-9446K761	24.00	24.00
High-Flow Perforated Sheet**	Must be cut to length. Used to replace the surface of the med-associates doors. Miniscopes, and similar head-stages, risk getting stuck in original med-associates social doors.	McMaster-Carr	1	92725T5-92725T23	62.55	125.10
Deadbolt	Locks main/social boxes	Reliabilt	2	3728814	3.98	5.96
Screws for floorgrids*	Attaches med-associates floorgrids to main chamber. SH8S075-8-32 Stainless Steel Cap Screw, 3/4″ Long, 50 Pack	Thorlabs	1 pack/50	SH8S075	8.33	8.33
Nuts for floorgrids*	Attaches med-associates floorgrids to main chamber. N8S0340-8-32 Stainless Steel Nut, 50 Pack	Thorlabs	1 pack/50	N8S0340	6.30	6.30
Washer for floorgrids	Attaches med-associates floorgrids to main chamber. W8S038 - #8 Washer, M4 Compatible, Stainless Steel, 100 Pack,	Thorlabs	1 pack/100	W8S038	3.86	3.86
Large screwdriver	Used for the larger McMaster screws (and Thorlabs screws)	Thorlabs	1	BD-2.5M	4.65	4.65
Small Screwdriver	Used for the smaller McMaster screws	Thorlabs	1	BD-4M	5.49	5.49
Cameras	Records behavior	FLIR	2	BFLY-PGE-12A2C-CS	355.00	710.00
Camera Cables	Power and data transfer from cameras	FLIR	2	ACC-01-3009	37.50	75.00
Camera attachment	Changes adapter to fit on rails: 26.9 mm by 17.9 mm, 1/4″−20 Tripod Adapter	FLIR	2	ACC-01-0003	11.80	23.60
TR2-P5 - Ø1/2″ Optical Post*, 5 pack	TR2-P5 - Ø1/2″ Optical Post, SS, 8–32 Setscrew, 1/4″−20 Tap, L = 2″. Connects cameras to rails. Need 2 per box	Thorlabs	2	TR2-P5	26.52	26.52
RA90-P5 - Right-Angle Clamp*	RA90-P5 - Right-Angle Clamp for Ø1/2″ Posts, 3/16″ Hex*, 5 Pack:	Thorlabs	1	RA90-P5	52.76	52.76
Network Card	Allows for up to 2 behavioral camera streams simultaneous	Amazon	1	ASIN: B01IR7T7PG	73.99	73.99
Sound attenuation chamber	Attenuates sounds for box	Amazon	1	ASIN: B00PJOL0FG	125.00	125.00
Overhead strip-lights	Illuminates box in multiple colored LEDs.	Amazon	1	ASIN: B08885ZJTQ	26.00	26.00
MEDPC: TTL adapter	28 V DC to TTL Adapter with BNC connector. Used for triggering camera frames.	Med Associates	2	SG-231	180.00	180.00
MEDPC: Social Door	Automatic Door for Social Chamber	Med Associates	1	ENV-010B2-SOC	622.00	622.00

All additional components required to make the box and associated configurations. It is suggested to build these boxes in batches larger than 1 so that maximum cost savings can be applied. Certain items on this list (denoted with*) indicate the ability to be used across more than 1 box. Other items are marked with** which means they are optional for other applications (i.e., perforated sheets are not necessary if doing pure behavior studies but are necessary for miniscope recordings). We estimate a total cost to build a single box (without cameras, Med Associates pieces) for 540.69. If adding the attachable social chamber, the additional cost (with Med Associates pieces) is 927.00 but the perforated sheet, for example, can be used for more than 10 boxes. If also adding dual-cameras, cables, network cards, and optical posts the additional cost is estimated at 1141.88 per box.

   c. Ensure that rail 14 is oriented such that one slotted face is towards the outside of the box and the other allows for an acrylic wall to slide into the door frame.
   d. Secure a door handle to rail 14 and a door hinge to rail 6. Slide in acrylic pF (Fig. 3).

Mounting cameras and configuring MedPC

To mount cameras onto the operant chamber, numerous configurations are made possible with the use of ThorLabs Ø1/2″ Optical Posts and Ø1/2″ Angle Post Clamps. Using 2 two-inch Ø1/2″ Optical Posts and a RA90 Ø1/2″ Angle Post Clamp, a FLIR camera
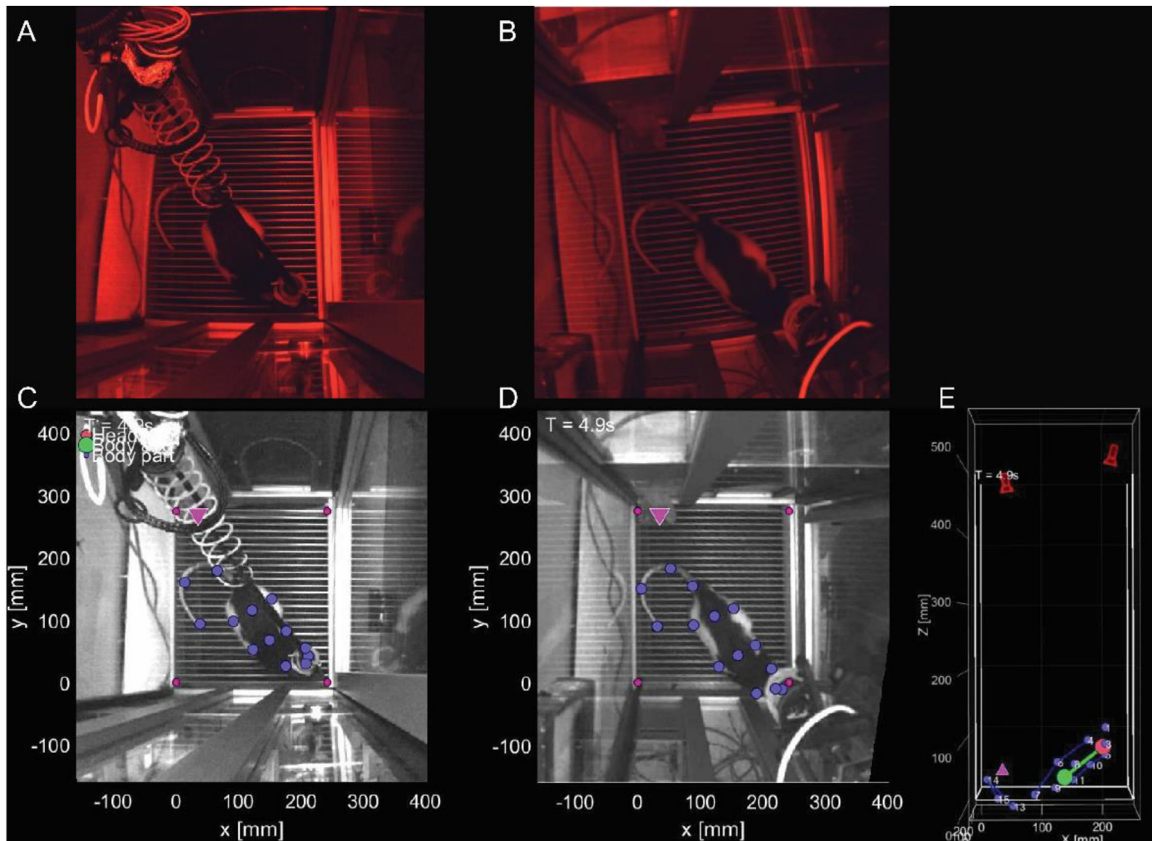
Fig. 7. Dual camera views and 3D reconstruction. Top (A, B): Raw video of the "FlyCapture" program set for recording single or dual-camera behavioral videos. In this setup, two cameras are placed at opposing corners of the chamber to facilitate 3D reconstruction. Ensure that the floorgrid of the chamber is at the center of each camera view. Consistent markings (e.g., an "X" on the acrylic walls) that is visible by both cameras is not shown but necessary for calibration purposes. Bottom (C, D, E): The same images seen in (A) and (B) are shown in (C) and (D). These are images corrected for any differences in camera orientation and position the floorgrid perfectly in each view. Also shown (E) is a reconstructed 3D configuration of automatically detected points using a DeepLabCut model. The position of the cameras can also be seen in (E). .

can be secured onto rails 2A-D with sufficient adjustability to provide a clear view of subject activity within the operant chamber. Additional cameras may be set up to provide complete viewing angles, perspectives, and 3D modeling of subject behavior to support deep learning capabilities. As shown in Fig. 7, two cameras are angled to center the floor with one in the front left corner and one in the back right corner of the chamber. The camera settings for dual camera setup in the FlyCapture program can be found in Table 4.

With the operant chamber assembled, it should be noted that the chamber allows for significant modification and application of various hardware components. With three sections on the left side of the box and a remaining fourth section on the right side, the operant chamber can be modified to support different experimental designs and orientations. Using the hardware and configuration described in assembly, wiring the operant chamber can be summarized in the following Fig. 8.

To coordinate MedPC with neural miniscope recordings and behavior video capture, modifications were made to the FLIR cable to allow this cable connection to provide power, trigger the camera as required by MedPC, and allow additional MedPC logging codes to be triggered and sent. A diagram of the modified cable is shown in Fig. 8 with a potential configuration to MedPC through two SG-231 MedPC control boxes and a neural mapper for miniscope coordination.

Discussion

Flexibility of the box design: operant behavior and conditioning

Operant chambers are traditionally small enclosures equipped with various hardware to present simplistic stimuli to collect data related to rat behavior. However, the design of typical commercial operant chambers restricts modifications which can limit the flexibility of their design. As a result, this inherently constrains the scope of potential experimentations. Our open-source operant chamber has been constructed to alleviate these issues and to accommodate a breadth of behavioral experiments.

Our chamber was designed to accommodate traditional operant lever-press style experiments including food [27] and drug self-administration [28]. The main structure has an open concept design which allows for the addition of a motorized commutator to

Table 4

Camera settings made in FlyCapture for dual-camera recording. Camera settings for multi-camera behavior recording using FlyCapture program and FLIR cameras.

Camera settings—Notes: Deactivate absolute mode			
	Value	Auto	On/Off
Brightness	0	–	–
Exposure	442	Off	On
Sharpness	1024	–	–
Hue	2048	–	–
Saturation	1024	–	–
Gamma	1024	–	–
Shutter	1000	Off	–
Gain	40	Off	–
Frame rate	480	Off	Off
W.B. (Red)	600	Off	On
W.B. (Blue)	693	–	–
Power	–	–	On/Off

Custom video modes		
		Value
Image	Left	0
	Width	1280
	Top	0
	Height	960
Binning	Horizontal	1
	Vertical	1
Packet size	9000	
Packet delay	3000	

Trigger / strobe control		
	Setting	
Enable/disable trigger	On	
Trigger source	GPIO 0	
Trigger polarity	High	
Trigger delay	Off	
Pin direction control	GPIO 0	In
	GPIO 1	Out
	GPIO 2	In
	GPIO 3	In

Advanced camera settings		
Raw Bayer output	Off	
Mirror image	Off	
Y16 endianness	Little endian	
Display test pattern	None	
Memory channels	Channel	Default
GigE packet resend	Enable	
Embedded image information	Select all	
Auto range control	Property	Exposure
	Min	256
	Max	768

assist in intravenous drug SA. This can be mounted onto rail 2D, which can be moved for Z axis adjustment. The commutator can be adjusted in any X or Y position by adjusting its location on rail 2D (Fig. 2; Top, Fig. 7). These types of adjustments can be made between rats of different sizes (e.g., for male or female rats) to prevent "pulling." In this sense, care can be taken so that individual differences like these can be accounted for and corrected in case issues arise.

Our attachable social attachment allows for social self-administration [23,24], drug/social "choice" [29,30] and drug/food choice [31]. The social chamber and social door are connected to the main chamber such that social self-administration and choice models including social self-administration are efficacious. This social attachment can be further modified to include a larger space (for social self-administration of multiple partners) which is completely restricted by typical commercial designs.

Our design allows for expansion of the box in ways commercial options are limited. For instance, sections of acrylic (and any standing rails) can theoretically be removed and replaced by various "touch-screens" [32,33] with minimal modifications to the overall design for presentation of specific stimuli or for additional types of response paradigms. Our box is designed where removing sections of walls still allows for free-standing boxes, while many commercial options will not maintain their structural integrity upon removing various walls and can completely collapse if modified in this way.
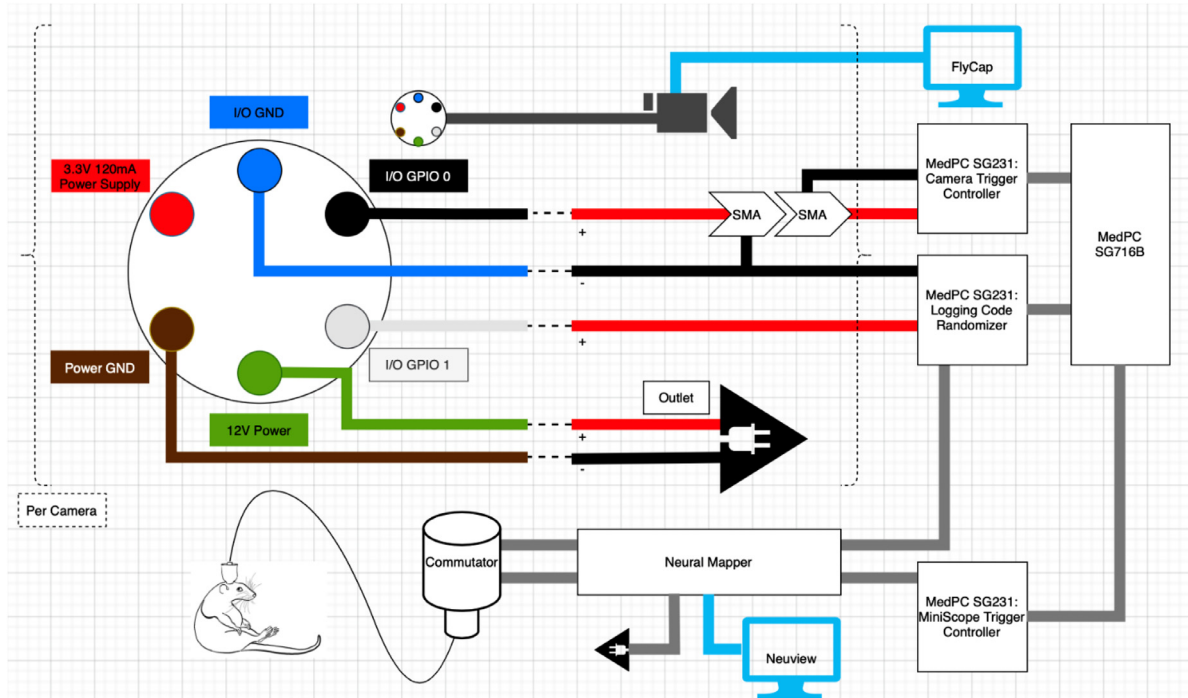
Fig. 8. Wiring diagram. Wiring diagram for synchronized behavior and neural recordings. Each FLIR camera requires a modified cable with soldered connections to a standard 110 V power outlet, a MedPC SG231 Camera Trigger controller, and a MedPC SG231 Logging Code randomizer. A neural mapper is additionally wired to the same randomizer to synchronize neural recordings with behavior videos. Each SG231 is linked to a MedPC SG-716B SmartCtrl Connection Panel to initiate behavior and neural recordings.

A function of our box that allows it to stand above traditional designs is this flexibility and "future-proofing" for any additional long term experiments. Our box is constructed in a format that allows for continual reconfiguration. The box has appropriate spacing to incorporate and remove each operant-based component described above quickly and efficiently. For example, within the main chamber each acrylic piece has been measured and cut to be size-compatible with each Med Associates instrument – in this format, a food-port can be easily replaced for a cue light, or an acrylic block without any foundational restructuring. This design emphasizes adaptability within behavioral experimentation and allows for long-term usage and customization which exceeds many commercial options. Both custom and commercial (Med Associates Inc.) components including levers, cue lights, social doors, and food/water ports—each of which is an essential component in traditional operant training can be added easily. The modular nature of the floorboards means we can also incorporate a med-associates "shock" enabled floor (part number: ENV-005A-T) for punishment-based operant experiments [34], drug self-administration in the presence of pain [35], and other behavioral paradigms.

Flexibility of the box design: in vivo recording techniques

Our box was designed with miniscope imaging as the primary experimental pursuit. However, any typical in vivo behavioral neuroscience procedure can be optimized for this style of box due to its long-term housing capabilities, cleanliness, and ability to mount external pieces such as cameras, commutators, and other sensitive equipment. Alternative neuroscience-based methods include paradigms such as 2-photon recordings, electrophysiology, microdialysis, optogenetics, and chemogenetics. Both 1- and 2-photon recordings provide valuable insight into the circuit level of neuronal interactions allowing for a deeper understanding of human brain function [5,17,36,37]. Both can require long stretches of delicate cables that run through the opening of the box and connect at the headstage of the animal (Video 2) and this box is designed to accommodate commutators that can adjust in height based on the requirements of the specific subject based on its X, Y, and Z location (adjustable by rail 2D).

In vivo electrophysiology utilizes steel wire to record changes in extracellular sodium concentration as a proxy for neuronal activity [38–40]. Like 1- and 2-photon recordings, this requires careful placement of wiring to avoid accidental damage from chewing. Microdialysis scans for changes in neurotransmitter levels in particular brain regions detailing the paracrine activity involved in different activities [41,42]. These tubes must also be carefully placed to avoid tangles and biting, but this box can easily accommodate this practice. Optogenetic experiments provide pinpoint precision in studying neural activity and its outcomes in specific subsets of cells using light-sensitive proteins called opsins [43]. Any external light-generating equipment can be easily mounted externally to the box to reduce strain on the delicate fiber optic cables.
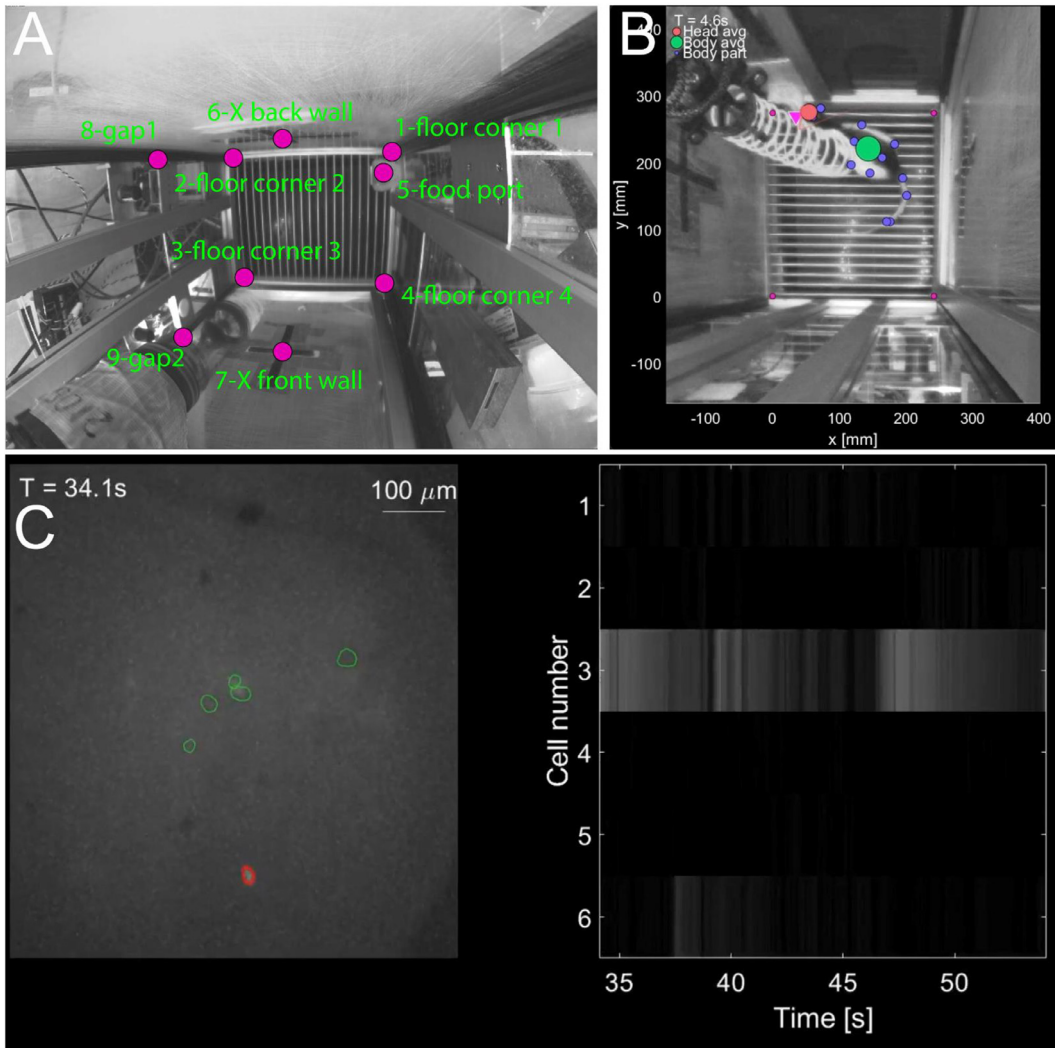
Fig. 9. Views of operant chamber. (A) Landmarks used for camera calibration to facilitate 3D reconstruction using depth of field. (B) Obstruction caused by various components. These can be avoided by moving cameras to "better" (i.e., less obstructed) locations within the box (C) Sample of poor quality neural data due to damage from a rat falling from climbing in a commercial operant box. The damage to the lens obscures (or kills) all neurons within the field of view, in comparison with Video 1 which shows the potential of 100+ neurons recorded from a single rat in vivo.

The commonality in each of these data collection techniques allows for a collection of potential behavioral changes via dual-camera setups (Fig. 7). Associated neural data can then be correlated to extract valuable relationships. While our box was not specifically designed for these experiments, it is imperative to recognize the value and flexibility this box can provide to expand the opportunities for the greater scientific community.

Benefits to long term housing in this operant chamber

The initial design of this operant chamber is optimized to support long-term miniscope in vivo imaging in rats while also mitigating many potentially detrimental risks. As mentioned above, these benefits can extend to other neuroscience in vivo techniques. For example, one such benefit provided by long term housing is to prolong the life of miniscope equipment. A standard practice in miniscope imaging (and similar techniques) is to only leave the miniscope on the subject's head for the duration of the experiment—administering anesthesia to remove the miniscope and change them between subjects. Repeated anesthesia administration can result in heightened anxiety [44]. In rats, this can lead to violent behaviors such as panicking, rolling, or jumping–resulting in particularly serious consequences such as damage to the miniscope, implanted GRIN lens, and brain. Fig. 9C demonstrates evidence of damage to a GRIN lens and subsequent scarring of internal brain tissue due to the animal climbing and falling in a commercially available box. In comparison with Video 1, Fig. 9C shows a 90% reduction of possible neurons achievable from our custom operant chamber. This is likely because rats are less likely to harm themselves, and their neurons, using our custom box.

A solution to this problem is to affix the miniscope to the rat's head for the entirety of the experiment. In this way, isoflurane exposure is minimized, which protects health and may help prolong the duration of neural recording. This creates an added benefit of retaining the exact focal plane of the GRIN lens for the entirety of the experiment and reduces reliance on algorithmic post-processing [45].

Long term housing in these operant chambers is more beneficial to the welfare of post-surgical animal subjects. Not only are these boxes larger than traditional shoebox cages, but they can also be fitted with water bottles, and can support a 24/7 light cycle using MedPC LED modules. Furthermore, these chambers are easier to sanitize than the sawdust environment of traditional shoebox cages. Traditional cage environments are insufficient for infection control, which could result in infections that lead to loss of the headcap and subsequently, that animal. Enrichment such as chew toys and paper towels may be provided to rats to improve comfort within the chambers without significantly reducing sanitation. By minimizing the chance of infections and the damage that could be done to the miniscope, headcap, and animal, this operant chamber improves the animal's welfare and maximizes data collection options.

Deep learning analysis of neural and behavioral data

Traditional 2D video tracking can be collected in this chamber with a top-down view, side view, a slightly angled view, or from the bottom up. However, 2D video tracking requires making assumptions regarding distortion as animals move away from the camera. A major benefit of this operant chamber is the highly modifiable arrangement of multiple cameras and angles (Fig. 7). Multiple cameras simplify depth-of-field calculations (Fig. 7C–E), allowing for various 3D reconstructions and increased accuracy in future analyses. Diverse camera views can minimize occlusions and enable the usage of 3D body part tracking in freely moving animals (Fig. 7E).

Additional rails may be attached to establish novel camera views both internal or external of the chamber. Transparent acrylic walls allow for unobstructed views of external cameras to the behavior subject. Bottom-up camera views may also be established with acrylic panel flooring.

One of the key advantages of the proposed custom setup is the ability to set up multiple cameras at the desired angle and configuration by securing them to the railings with optical posts (Table 3). This allows both a flexible multi-view configuration (from different angles of the acrylic box, including sides and underneath), and a stable camera positioning, which is crucial for accurate tracking results. Although multi-camera setups offer a much deeper level of detail in the behavior analysis and neural correlates compared with overhead single camera setups, there are some important aspects to consider: Despite the stable mounting of the cameras, occasional change in orientation is likely to occur during behavioral task recordings or during routine maintenance operations.

To ensure accurate results, it is important to address these changes in camera view angles, which can be done either by automatic landmark detection (e.g. through DeepLabCut), or by manually detecting landmarks when changes in orientation are detected (Fig. 9A). Another factor which could hinder the quality of 3D reconstruction is the occlusion of tracked body parts, either by external hardware (e.g. cables, commutators, etc.) or by the rodent's body (Fig. 9B). This issue can be effectively addressed through an accurate choice of camera positioning, which minimizes obstruction of the animal as it performs the specific behavioral task (Video 1). Additionally, it is important to consider the increase in computational resources needed to process the data, both in terms of capacity (for the larger number of video streams recorded) and computational power required for body part detection, filtering, 3D reconstruction and neural correlate analysis.

With multiple cameras, experimenters can train a network for each camera view or train a network that generalizes to multiple camera views.

Quantifying behavior with deep learning approaches is a key component in modeling longitudinal animal behavior [46]. This can be done with models such as DeepLabCut, which tracks location and posture across video frames [47]. Pose estimation can be further analyzed with behavior classification algorithms such as PyRAT, HubDT, and deep behavior mapping (DBM) [6,48–50]. DBM is used to capture behavioral microstates on a moment-to-moment basis [6]. These algorithms split long-term behavioral data into stereotyped behavior trends, breaking them into segmented points of repeated behaviors such as trials during operant behavior. The stereotyped movements can be grouped into distinct segments and correlated with neural data and tracked over time. Specific neural populations can be manipulated to observe changes in neural activity and any differences in associated behaviors.

Increased accuracy in tracking data results in increased accuracy in longitudinal behavior modeling, allowing for precise connections to be made between behavior and neural activity. Distinct neuron populations can be associated with unique behaviors. One study explored differences in morphine vs. drug free behavior using multi-dimensional behavioral analyses. They found different associations in anterior cingulate neuronal firing between the two states [48]. Other examples of behaviors that can be analyzed with deep learning include differences between behavioral responses, choices, and rewards (i.e. drugs vs. social or food vs. social). The correlation of such behaviors can be associated with neural data from brain regions of interest. Ultimately, deep learning tools can be leveraged to identify associations between neural and behavior data over long periods of time, expanding the possibilities for breakthroughs in behavioral neuroscience on a more detailed and accurate scale that few other techniques have been able to achieve.

Conclusion

The design of this operant chamber is an optimized method to utilize long-term miniscope in vivo imaging in rats. The top of the chamber is left open and is customizable using various size acrylic pieces. This provides space for cables and other equipment that can be connected from the animal to the outside of the box for neural recordings, drug delivery, and other in vivo behavioral neuroscience techniques. The acrylic walls and rails allow for flexible camera placement, which is beneficial for deep learning analyses of behavioral

video data. The modifiable nature of the operant chamber enables simultaneous multidimensional behavioral recordings and in vivo neural recordings such as 1-photon calcium imaging using miniscopes (Video 1) but can be adapted for use with a host of modern in vivo behavioral neuroscience methodologies with ease. Additionally, our operant chambers also allow for long-term housing of rats, which can improve animal welfare and reduce the amount of damage to rats and their miniscopes. Overall, our operant chambers are customizable, adaptable within behavioral experimentation, and long-lasting, making them a great option for a breadth of behavioral neuroscience experiments.

Appendix

Reversing corner concealed brackets

Corner concealed brackets secure to two slotted faces of perpendicular rails by tensioning screws against the inner core of each rail. However, these brackets may conflict with acrylic walls that also need to sit in the slots of certain rails. As such, specific circumstances require reversing one tension screw by removing it completely and reinserting it in the opposite direction. One tension screw of a corner concealed bracket is reversed to secure rail 2A to rail 1A which accommodates for the space required by the acrylic walls.

Preparing the social guillotine door

To prepare the social chamber door, two parts of the Med Associates social guillotine door will need to be removed: the upper horizontal plate and the lower door stopper (Fig. 6). While the door stopper can be removed directly, the metal barrier and plastic portal frame on either side of the guillotine door will need to be temporarily detached. Reattach the silver barrier and plastic portal frame afterward.

Ethics statements

All experiments were conducted in accordance with the guidelines of Institutional Animal Care and Use.

Funding

Declaration of competing interests

The authors declare that they have no known competing financial interests or personal relationships that could have appeared to influence the work reported in this paper.

CRediT authorship contribution statement

Nicholas J. Beacher: Conceptualization, Methodology, Software, Validation, Writing – original draft, Writing – review & editing, Visualization, Supervision, Project administration. **Jessica Y. Kuo:** Methodology, Validation, Writing – original draft, Writing – review & editing, Visualization. **Miranda Targum:** Methodology, Validation, Writing – original draft, Writing – review & editing, Visualization. **Michael Wang:** Methodology, Validation, Writing – original draft, Writing – review & editing, Visualization. **Kayden A. Washington:** Methodology, Validation, Writing – original draft, Writing – review & editing, Visualization. **Giovanna Barbera:** Methodology, Software, Validation, Writing – original draft, Writing – review & editing, Visualization, Supervision, Project administration. **Da-Ting Lin:** Methodology, Validation, Writing – original draft, Writing – review & editing, Supervision, Project administration, Resources, Funding acquisition.

Data availability

I have shared a link to all code used in the paper and is linked in the main manuscript.

Acknowledgments

Supplementary materials

Supplementary material associated with this article can be found, in the online version, at doi:10.1016/j.mex.2024.102721.

References

[1] N.J. Beacher, K.A. Washington, Y. Zhang, Y. Li, D.-T. Lin, GRIN lens applications for studying neurobiology of substance use disorder, Addict. Neurosci. 4 (2022) 100049.

[2] G. Barbera, et al., Spatially compact neural clusters in the dorsal striatum encode locomotion relevant information, Neuron 92 (1) (2016) 202–213, doi:10.1016/j.neuron.2016.08.037.

[3] G. Barbera, B. Liang, L. Zhang, Y. Li, D.T. Lin, A wireless miniScope for deep brain imaging in freely moving mice, J. Neurosci. Methods 323 (2019,) 56–60, doi:10.1016/j.jneumeth.2019.05.008.

[4] B. Liang, et al., Distinct and dynamic ON and OFF neural ensembles in the prefrontal cortex code social exploration, Neuron (2018), doi:10.1016/j.neuron.2018.08.043.

[5] L. Zhang, et al., Miniscope GRIN lens system for calcium imaging of neuronal activity from deep brain structures in behaving animals, Curr. Protoc. Neurosci. 86 (1) (2019) e56, doi:10.1002/cpns.56.

[6] Y. Zhang, et al., Detailed mapping of behavior reveals the formation of prelimbic neural ensembles across operant learning, Neuron 110 (4) (2022) 674–685 e6.

[7] K.-S. Chen, et al., A hypothalamic switch for REM and non-REM sleep, Neuron 97 (5) (2018) 1168–1176 e4.

[8] K.K. Ghosh, et al., Miniaturized integration of a fluorescence microscope, Nat. Methods 8 (10) (2011) 871–878, doi:10.1038/nmeth.1694.

[9] A.M. Stamatakis, et al., Miniature microscopes for manipulating and recording in vivo brain activity, Microscopy 70 (5) (2021) 399–414.

[10] J.C. Jimenez, et al., Anxiety cells in a hippocampal-hypothalamic circuit, Neuron 97 (3) (2018) 670–683 e6.

[11] A. Klaus, G.J. Martins, V.B. Paixao, P. Zhou, L. Paninski, R.M. Costa, The spatiotemporal organization of the striatum encodes action space, Neuron 95 (5) (2017) 1171–1180 e7.

[12] B. Liang, et al., Striatal direct pathway neurons play leading roles in accelerating rotarod motor skill learning, Iscience 25 (5) (2022) 1–17.

[13] E.E. Hart, G.J. Blair, T.J. O'Dell, H.T. Blair, A. Izquierdo, Chemogenetic modulation and single-photon calcium imaging in anterior cingulate cortex reveal a mechanism for effort-based decisions, J. Neurosci. 40 (29) (2020) 5628–5643.

[14] F. Gobbo, et al., Neuronal signature of spatial decision-making during navigation by freely moving rats by using calcium imaging, Proc. Natl. Acad. Sci. 119 (44) (2022) e2212152119.

[15] H.S. Wirtshafter, J.F. Disterhoft, In vivo multi-day calcium imaging of CA1 hippocampus in freely moving rats reveals a high preponderance of place cells with consistent place fields, J. Neurosci. 42 (22) (2022) 4538–4554.

[16] C. Guo, et al., Miniscope-LFOV: a large-field-of-view, single-cell-resolution, miniature microscope for wired and wire-free imaging of neural dynamics in freely behaving animals, Sci. Adv. 9 (16) (2023) eadg3918.

[17] G. Barbera, Y. Zhang, C. Werner, B. Liang, Y. Li, D.-T. Lin, An open source motorized swivel for in vivo neural and behavioral recordings, MethodsX 7 (2020) 101167.

[18] S. Sheshadri, B. Dann, T. Hueser, H. Scherberger, 3D reconstruction toolbox for behavior tracked with multiple cameras, J. Open Source Softw. 5 (45) (2020) 1849.

[19] H. Hu, R. Zhang, T. Fong, H. Rhodin, T.H. Murphy, Standardized 3D test object for multi-camera calibration during animal pose capture, Neurophotonics 10 (4) (2023) 046602.

[20] I. Sarkar, I. Maji, C. Omprakash, S. Stober, S. Mikulovic, and P. Bauer, "Evaluation of deep lift pose models for 3d rodent pose estimation based on geometrically triangulated data," *arXiv preprint* arXiv:2106.12993, 2021.

[21] T. Nath, A. Mathis, A.C. Chen, A. Patel, M. Bethge, M.W. Mathis, Using DeepLabCut for 3D markerless pose estimation across species and behaviors, Nat. Protoc. 14 (7) (2019) 2152–2176.

[22] R. Escobar, B. Gutiérrez, R. Benavides, 3D-printed operant chambers for rats: design, assembly, and innovations, Behav. Processes 199 (2022) 104647.

[23] J.J. Chow, et al., Characterization of operant social interaction in rats: effects of access duration, effort, peer familiarity, housing conditions, and choice between social interaction vs. food or remifentanil, Psychopharmacology 239 (2022) 1–16.

[24] M. Venniro, Y. Shaham, An operant social self-administration and choice model in rats, Nat. Protoc. 15 (4) (2020) 1542–1559.

[25] N.J. Beacher, et al., Circuit investigation of social interaction and substance use disorder using miniscopes, Front. Neural Circuits 15 (2021) 762441.

[26] S.R. White, L.M. Amarante, A.V. Kravitz, M. Laubach, The future is open: open-source tools for behavioral neuroscience research, eNeuro 6 (4) (2019) 1–5.

[27] M.S. Cousins, J.D. Sokolowski, J.D. Salamone, Different effects of nucleus accumbens and ventrolateral striatal dopamine depletions on instrumental response selection in the rat, Pharmacol. Biochem. Behav. 46 (4) (1993) 943–951.

[28] R.A. Yokel, R. Pickens, Drug level of D-and L-amphetamine during intravenous self-administration, Psychopharmacologia 34 (3) (1974) 255–264.

[29] M. Venniro, T.I. Russell, M. Zhang, Y. Shaham, Operant social reward decreases incubation of heroin craving in male and female rats, Biol. Psychiatry 86 (11) (2019) 848–856.

[30] M. Venniro, et al., Volitional social interaction prevents drug addiction in rat models, Nat. Neurosci. 21 (11) (2018) 1520–1529, doi:10.1038/s41593-018-0246-6.

[31] E.A. Townsend, K.L. Schwienteck, H.L. Robinson, S.T. Lawson, M.L. Banks, A drug-vs-food "choice" self-administration procedure in rats to investigate pharma-cological and environmental mechanisms of substance use disorders, J. Neurosci. Methods 354 (2021) 109110.

[32] G. Barbera, B. Liang, Y. Zhang, C. Moffitt, Y. Li, D.T. Lin, An open-source capacitive touch sensing device for three chamber social behavior test, MethodsX 7 (2020) 101024, doi:10.1016/j.mex.2020.101024.

[33] T.J. Bussey, T.L. Padain, E.A. Skillings, B.D. Winters, A.J. Morton, L.M. Saksida, The touchscreen cognitive testing method for rodents: how to get the best out of your rat, Learn. Memory 15 (7) (2008) 516–523.

[34] M. Broomer, N. Beacher, M.W. Wang, and D.-T. Lin, "Examining a punishment-related brain circuit with miniature fluorescence microscopes and deep behavior mapping," Available at SSRN 4623000.

[35] T.J. Martin, E. Ewan, Chronic pain alters drug self-administration: implications for addiction and pain mechanisms, Exp. Clin. Psychopharmacol. 16 (5) (2008) 357.

[36] O.A. Oghifobibi, et al., Resuscitation with epinephrine worsens cerebral capillary no-reflow after experimental pediatric cardiac arrest: an in vivo multiphoton microscopy evaluation, J. Cereb. Blood Flow Metab. 42 (12) (2022) 2255–2269.

[37] Y. Zhang, et al., Detailed mapping of behavior reveals the formation of prelimbic neural ensembles across operant learning, Neuron 110 (2021) 674–685.

[38] M. Pachitariu, N. Steinmetz, S. Kadir, M. Carandini, Kilosort: realtime spike-sorting for extracellular electrophysiology with hundreds of channels, BioRxiv (2016) 061481, doi:10.1101/061481.

[39] K.R. Coffey, et al., Electrophysiological evidence of alterations in the nucleus accumbens and dorsolateral striatum during chronic cocaine self-administration, Eur. J. Neurosci. 41 (12) (2015) 1538–1552.

[40] D.J. Estrin, J.M. Kulik, N.J. Beacher, A.P. Pawlak, S.D. Klein, M.O. West, Acquired alterations in nucleus accumbens responsiveness to a cocaine-paired discrim-inative stimulus preceding rats' daily cocaine consumption, Addict. Neurosci. 8 (2023) 100121.

[41] I. Filla, et al., Striatal dopamine D2 receptors regulate effort but not value-based decision making and alter the dopaminergic encoding of cost, Neuropsychophar-macology 43 (11) (Oct 2018) 2180–2189, doi:10.1038/s41386-018-0159-9.

[42] C. Biesdorf, et al., Dopamine in the nucleus accumbens core, but not shell, increases during signaled food reward and decreases during delayed extinction, Neurobiol. Learn. Mem. 123 (Sep 2015) 125–139, doi:10.1016/j.nlm.2015.06.002.

[43] K. Deisseroth, Optogenetics, Nat. Methods 8 (1) (2011) 26–29.

[44] K. Coleman, et al., Isoflurane anesthesia has long-term consequences on motor and behavioral development in infant rhesus macaques, Anesthesiology 126 (1) (2017) 74–84.

[45] A. Giovannucci, et al., CaImAn an open source tool for scalable calcium imaging data analysis, Elife 8 (2019) e38173.

[46] J.Y. Kuo, et al., Using deep learning to study emotional behavior in rodent models, Front. Behav. Neurosci. 16 (2022) 1044492.

[47] A. Mathis, et al., DeepLabCut: markerless pose estimation of user-defined body parts with deep learning, Nat. Neurosci. 21 (9) (2018) 1281–1289.

[48] A. Lindsay and J.K. Seamans, "HUB-DT: a tool for unsupervised behavioural discovery and analysis," *bioRxiv,* p. 2024.01.08.574696, 2024.

[49] A.J. Lindsay, I. Gallello, B.F. Caracheo, and J.K. Seamans, "Reconfiguration of Behavioral Signals in the Anterior Cingulate Cortex based on Emotional State," *bioRxiv,* p. 2023.07.12.548701, 2023.

[50] T.F. De Almeida, B.G. Spinelli, R. Hypolito Lima, M.C. Gonzalez, A.C. Rodrigues, PyRAT: an open-source python library for animal behavior analysis, Front. Neurosci. 16 (2022) 779106.